

ACTIVE MEDIA

PACS numbers: 42.55.Lt; 34.50.Gb; 52.40.Mj
DOI: 10.1070/QE2013v043n08ABEH015129

Quenching of krypton atoms in the metastable $5s(^3P_2)$ state in collisions with krypton and helium atoms

D.A. Zayarnyi, A.Yu. L'dov, I.V. Kholin

Abstract. **We have used the absorption probe method to study the processes of collisional quenching of the metastable 5s $[3/2]_2^o(^3P_2)$ state of the krypton atom in electron-beam-excited high-pressure He–Kr mixtures with a low content of krypton. The rate constants of plasma-chemical reactions $Kr^* + Kr + He \to Kr_2^* + He$ $[(2.88 \pm 0.29) \times 10^{-33}\ cm^6\ s^{-1}]$, $Kr^* + 2He \to HeKr^* + He$ $[(4.6 \pm 1.3) \times 10^{-36}\ cm^6\ s^{-1}]$ and $Kr^* + He \to products + He$ $[(1.51 \pm 0.15) \times 10^{-15}\ cm^3\ s^{-1}]$ are measured for the first time. The rate constants of similar reactions in the Ar–Kr mixture are refined.**

Keywords: *inert gases, krypton, helium, argon, plasma chemistry, quenching of atoms, absorption spectroscopy.*

1. Introduction

In this paper, we study experimentally plasma-chemical reactions of collisional quenching of excited 5s states of krypton atoms in high-pressure He–Kr mixtures. These experiments, in turn, are a continuation of our research on quenching processes of lower s states of heavy inert gases – xenon, neon and krypton – in their high-pressure mixtures ($p > 1$ atm) with lighter inert buffer gases (see reviews [1, 2] and references therein, and more recent publications [3–5]).

The present paper is devoted to measurement of quenching rate constants of Kr atoms in the lowest of the excited states – metastable $5s[3/2]_2^o$ ($^3P_2$) state (see Fig. 1) – in dense mixtures of Kr with the buffer gas He. We have studied the practically important high-pressure He–Kr mixtures with a small relative content of Kr, excited by a beam of fast electrons.

Currently in the literature the quantitative data on such processes are completely absent, despite the fact that they play an important role in forming the population inversion in high-pressure lasers on atomic transitions in inert gases [6, 7] and krypton dimer lasers [8].

At high pressures ($p = 1$–4 atm), atoms in the studied low-lying states are quenched in reactions involving collisions of three and two particles:

$$Kr^* + Kr + He \to Kr_2^* + He, \quad (1)$$

D.A. Zayarnyi, A.Yu. L'dov, I.V. Kholin P.N. Lebedev Physics Institute, Russian Academy of Sciences, Leninsky prosp. 53, 119991 GSP-1 Moscow, Russia; e-mail: kholin@sci.lebedev.ru

Received 17 January 2013; revision received 21 March 2013
Kvantovaya Elektronika **43** (8) 720–724 (2013)
Translated by I.A. Ulitkin

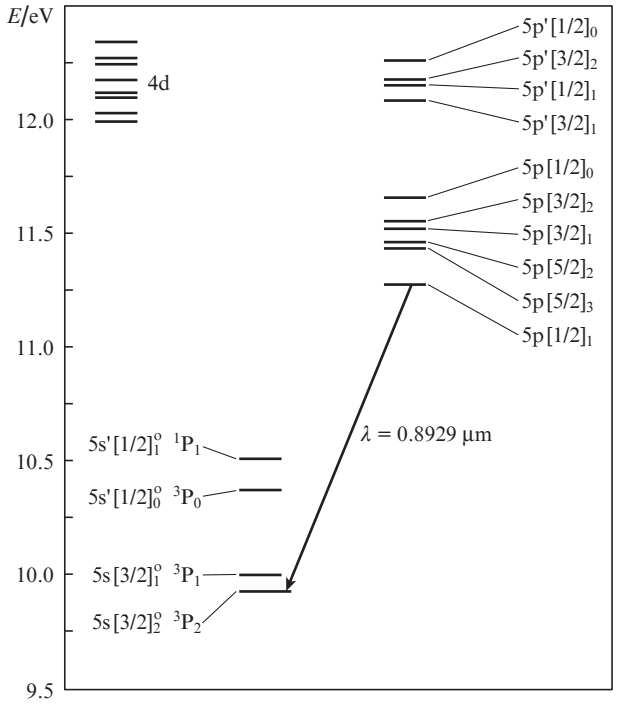

Figure 1. Diagram of the excited levels of a krypton atom.

$$Kr^* + 2He \to HeKr^* + He, \quad (2)$$

$$Kr^* + He \to products + He. \quad (3)$$

In determining the rate constant of reaction (3), we should bear in mind that the value obtained in the experiment is an upper bound, because it is also needed to take into account the reactions of excited krypton with atoms and molecules of impurities M in the gas mixture in question (mainly in He):

$$Kr^* + M \to products. \quad (4)$$

The relative concentrations m of different impurities in purified He are low (see below), but due to the large cross sections, the contribution of such reactions can be considerable.

For comparison, in this series of experiments we have also measured the rate constants of similar reactions in Ar–Kr mixtures studied in our previous works [3, 4]

$$Kr^* + Kr + Ar \to Kr_2^* + Ar, \quad (5)$$

$$Kr^* + 2Ar \to ArKr^* + Ar, \quad (6)$$

$$Kr^* + Ar \rightarrow \text{products} + Ar. \quad (7)$$

The rate constants have been measured by the absorption probe method [1, 2] from the dependence of the decay time of the states under study on the pressure and concentration ratio of the components of the working and buffer gases. To this end, in the afterglow of a high-power beam of fast electrons we have investigated the dynamics of absorption of a transmitting light pulse at a wavelength of 0.8929 μm, corresponding to a high-oscillator strength optical transition between one of the upper ($5p[1/2]_1$) levels of krypton and the metastable $5s[3/2]_2^o$ level in question (see Fig. 1).

2. Experimental setup

The experiments were performed by using a cold-cathode laser from an electron gun of a Tandem pulsed laser system [9]. The 250-keV pulsed electron beam of cross section 5×100 cm with a bell-shaped current pulse of base duration 2.5 ms was directed into a measuring chamber perpendicular to its optical axis through a 20-μm-thick titanium foil. The electron current density was 1.5 A cm^{-2}. The measuring chamber with an active volume of 5 L was made of stainless steel. Before filling with the gases under study, the chamber was evacuated via a nitrogen trap down to a residue pressure of ~10^{-5} Torr; the gas leaking into the chamber did not exceed 10^{-3} Torr h^{-1}. The mixtures of high-purity helium (purity 99.995%) and high-purity krypton (purity 99.9992%) with component ratios He : Kr = 50 : 1, 40 : 1 and 25 : 1 at pressures 1.75–4.0 atm were investigated. For comparison we also studied the mixture Ar : Kr = 200 : 1, 100 : 1 and 50 : 1 (see details in [3, 4]).

The optical scheme of absorption measurements is presented in Fig. 2. A broadband ISI-1 pulsed light source (*1*) emitting ~30-μs pulses [Fig. 3, curve (*2*)] produced probe radiation. At the source output, probe radiation was collimated into a beam of diameter 5 cm and, after passing through the measuring chamber (*5*) with the mixture under study, was focused on the entrance slit of a high-aperture ratio MDR-2 monochromator (*8*) with a 600-lines mm^{-1} grating acting as a dispersive element. The radiation transmitted through the monochromator set to the wavelength in question was focused on a photodetector (*10*) consisting of a fast BPW34 pin photodiode (Infinion) and a broadband AD8055 operational amplifier (Analog Devices) placed inside a doubly screened metal housing. Radiation in the second diffraction order was suppressed with a KS-10 optical filter (*3*) mounted at the output of the ISI-1 radiation source. Part of the radiation reflected from a plane-parallel glass plate (*4*) mounted in front of the measuring chamber was fed (bypassing the measuring chamber) to the entrance slit of an DMR-4 monochromator (*9*) and to the second photodetector (*11*). The output signals of the photodetectors were recorded with a two-channel digital DSO-2010 oscilloscope (Link Instruments) connected with a computer.

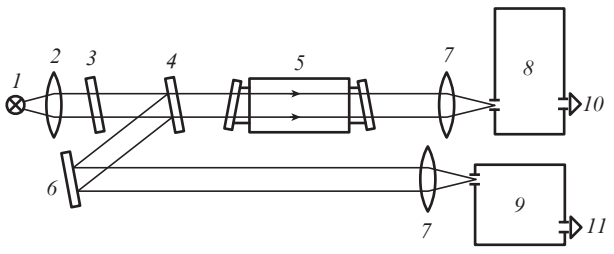

Figure 2. Optical scheme of absorption measurements: (*1*) ISI-1 pulsed light source; (*2*) collimating lens; (*3*) KS-10 optical filter; (*4*) beamsplitter; (*5*) measuring chamber; (*6*) fold mirror; (*7*) focusing lenses; (*8*) high-aperture ratio MDR-2 monochromator; (*9*) DMR-4 monochromator; (*10*, *11*) photodetectors.

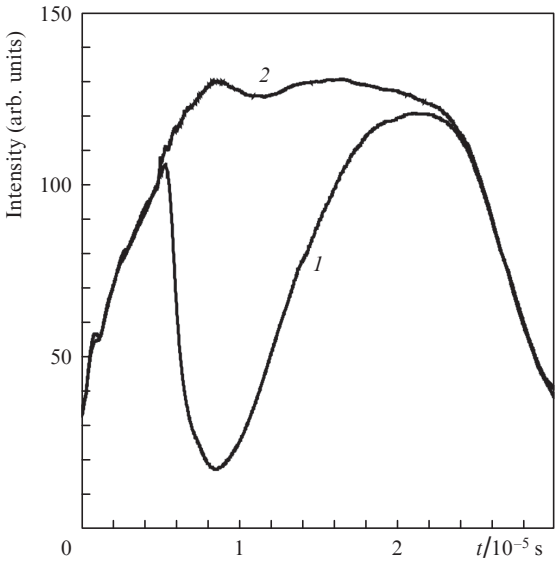

Figure 3. Time dependence of the intensity of the 0.893-μm ISI-1 radiation source, transmitted through (*1*) the measuring chamber and (*2*) around it, for the He : Kr = 50 : 1 mixture at a pressure of 2.5 atm.

Thus, the measuring scheme allowed us to record the shape and amplitude of the probe pulse simultaneously in front and behind an absorbing medium with the time resolution no worse than 100 ns.

3. Experiment and discussion

Excitation of the He–Kr mixtures by a beam of fast electrons leads to ionisation and excitation of atoms (mainly buffer gas He). At high pressures in the chains of plasma-chemical reactions of types

$$He^+ + 2He \rightarrow He_2^+ + He, \quad (8)$$

$$He_2^+ + Kr \rightarrow Kr^+ + 2He, \quad (9)$$

$$Kr^+ + Kr + He \rightarrow Kr_2^+ + He \quad (10)$$

excitation is transferred to molecular ions of krypton. The dissociative recombination of these ions with electrons

$$Kr_2^+ + e \rightarrow Kr^{**} + Kr \quad (11)$$

results in the formation of krypton atoms in different highly excited states, which then rapidly relax in collisions with heavy particles and secondary electrons, and in the radiative decay to the lower excited 5s states of the Kr atom.

In the afterglow of the electron beam pulse, during the completion of recombination and relaxation processes the concentration of Kr* in the state investigated in the present

work should be determined primarily by the processes of its decay in reactions (1)–(4):

$$\frac{d[Kr^*]}{dt} = -k_1[Kr][He][Kr^*] - k_2[He]^2[Kr^*] - (k_3 + k_4 m)[He][Kr^*]. \quad (12)$$

This time dependence of the concentration of Kr^* can be represented as an exponential

$$[Kr^*](t) = N_0 \exp(-k_d t) \quad (13)$$

with a decay rate

$$k_d = k_1[Kr][He] + k_2[He]^2 + (k_3 + k_4 m)[He]. \quad (14)$$

When the excited medium is probed by monochromatic radiation at the wavelength of the transition from a highly excited state to the state in question, the absorption coefficient k should be proportional to the concentration of atoms in this state:

$$k(t) \sim [Kr^*](t). \quad (15)$$

In our case, with the size of the input and output slits of the MDR-2 monochromator equal to ~0.2 mm, providing a satisfactory signal-to-noise ratio in the measurement path, the width of the instrument function of the monochromator in the pressure range 1.75 to 4.0 atm considerably exceeds the linewidth of the observed optical transition. In this situation, the Bouguer–Lambert–Beer law, generally speaking, is not valid, and one needs to use the empirical, or so-called modified, form of the Bouguer–Lambert–Beer law [10, 11], relating the measured transmittance T with the absorption coefficient k by the expression

$$\ln(1/T) = (kL)^\gamma. \quad (16)$$

Here, L is the length of the absorbing medium excited by the electron beam and γ is a dimensionless factor that depends on the ratio of the widths of the absorption line and the instrumental function of the monochromator. The study of the experimental dependences

$$\ln\ln[1/T(L)] = \text{const} + \gamma \ln L \quad (17)$$

confirmed the applicability of the modified Bouguer–Lambert–Beer law and allowed one to determine the dimensionless factor γ, equal to 0.5, in our experimental conditions (see [12]).

It follows from expression (16) taking into account relations (15) and from the expected time dependence $[Kr^*](t)$ (13) that the trailing edge of the 'absorption pulse' $\ln(1/T)$ should be purely exponential:

$$\ln[1/T(t)] \sim \exp(-\gamma k_d t). \quad (18)$$

Taking the logarithm of expression (18) leads to the following time dependence of transmittance T in the afterglow:

$$\ln\ln[1/T(t)] = \text{const} - \gamma k_d t. \quad (19)$$

Figure 3 shows typical pulse oscillograms of the ISI-1 source at the wavelength of the $5p[1/2]_1 - 5s[3/2]_2^o$ transition at the input and output of the measuring chamber filled with a He : Kr = 50 : 1 mixture at a pressure of 2.5 atm. By comparing the amplitudes of the signals at the input and output of the excited active medium, we can determine at each instant of time the transmittance T of the medium at the wavelength to which the monochromator is tuned. Figure 4 presents the time dependence of the absorption pulse $\ln(1/T)$ in the excited He–Kr mixture obtained from the oscillograms in Fig. 3 [curve (*1*)]. For comparison, Fig. 4 also shows the pulse $\ln(1/T)$ [curve (*2*)] obtained under similar experimental conditions for the Ar–Kr mixture. Noteworthy is the lengthening of the trailing edge of the pulse absorption (*1*), indicating a significant slowdown of abnormally slow processes of collisional quenching when the He–Kr mixture is used instead of the Ar–Kr mixture [3, 4].

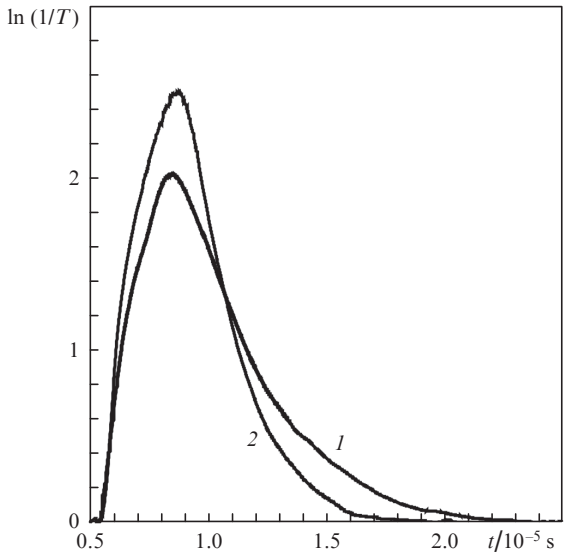

Figure 4. Time dependences of the absorption pulses $\ln(1/T)$ for (*1*) He : Kr = 50 : 1 and (*2*) Ar : Kr = 50 : 1 mixtures at a pressure of 2.5 atm.

Figure 5 shows for the oscillograms of Fig. 3 the time dependence of the function $\ln\ln(1/T)$ for the trailing edge of the absorption pulse. One can see that the approximation of the dependence of the linear function of type

$$\ln\ln(1/T) = p - \gamma k_d t \quad (20)$$

[curve (*1*)] does not lead to satisfactory results. This is explained by the fact [3, 4] that due to the small collisional quenching rates of $Kr^*(6s)$ levels, it is necessary to take into account the influence of even weak recombination fluxes, which continue to populate the level in question in the afterglow after the end of the electron pump pulse, on their populations. In the experiment, the influence of the recombination effect noticeably differs from the exponential time dependence of the trailing edges of the absorption pulse $\ln(1/T)$ (Fig. 4) and, therefore, demonstrates the nonlinear time dependence of $\ln\ln(1/T)$ (Fig. 5), which is different from (20).

To find the exponential component of the trailing edge of the absorption pulse, the time dependences were processed

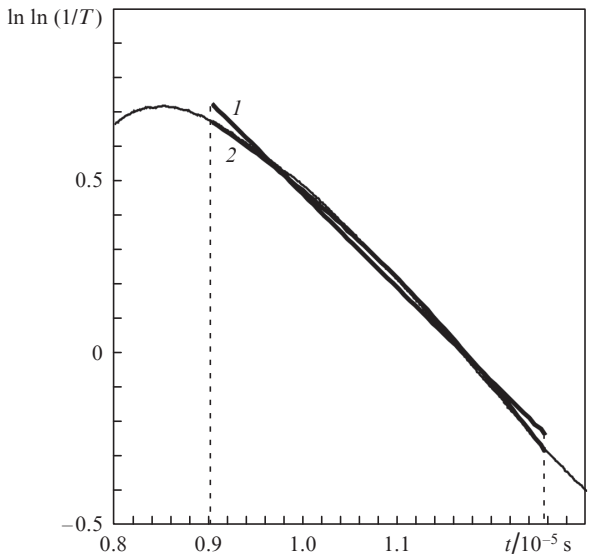

Figure 5. Time dependence of the function $\ln\ln(1/T)$, corresponding to the signals in Fig. 3, approximated by (*1*) (thick lines) the straight line and (*2*) the second-order curve.

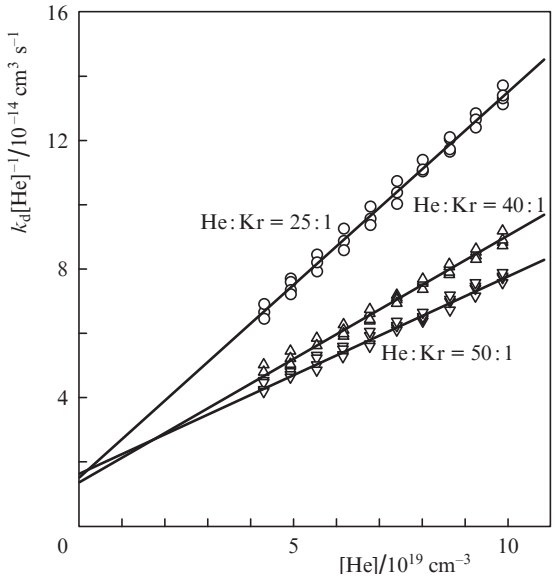

Figure 6. Dependences of the reduced quenching rates $k_d[He]^{-1}$ on the helium concentration in different He–Kr mixtures.

numerically using their approximation by a quadratic polynomial

$$\ln\ln(1/T) = p - (\gamma g)^2(t - t_0)^2 - \gamma k_d t(t - t_0) \quad (21)$$

(p, g and k_d are the approximation parameters; the time t_0 is measured from the end of the pump pulse), in which the linear part determines the required collisional quenching rate k_d, while the small quadratic correction is related to the population dynamics of the level.

The quenching rates from the experimental time dependences $\ln\ln(1/T)$ were calculated with the help of the least squares method with varying coefficients p, g and k_d by using the Levenberg–Marquardt algorithm [13]. A set of the experimental data for the mixtures He : Kr = 25 : 1, 40 : 1, 50 : 1 and Ar : Kr = 50 : 1, 100 : 1, 200 : 1 was processed at pressures from 1.75 to 4.0 atm with a step of 0.25 atm.

In the coordinates of Fig. 4 function (21) corresponds to the function

$$\ln\ln(1/T) = \exp(p)\exp[-(\gamma g)^2(t - t_0)^2]\exp[-\gamma k_d(t - t_0)], \quad (22)$$

which is a superposition of the exponential, which describes the collisional quenching, and the Gaussian pre-exponential, which gives a correction for recombination and relaxation processes. Determination of the real form of the pre-exponential in the analytical form is hardly possible because of the variety and complexity of its reactions, depending, in particular, on the time-varying temperature and density of the secondary electrons. However, in practice such a 'mnemonic' description in the dynamic range of variations in the transmittance $T = 0.1–0.9$ (see Fig. 3) gives satisfactory results. For example, for each He–Kr mixture Fig. 6 presents the dependences of $k_d[He]^{-1}$, i.e., the quenching rate reduced to the concentration of He, on the concentration of this buffer gas. In this case, according to the linear dependences

$$k_d[He]^{-1} = (\delta k_1 + k_2)[He] + (k_3 + k_4 m) \quad (23)$$

which follows from (14) (δ = [Kr]/[He] is the relative content of krypton in the mixture), the experimental points with good accuracy lie on the straight lines originating from a common point on the ordinate axis, which indicates the adequacy of representation (22) and the correctness of the procedure of experimental data processing.

The thus obtained set of experimental values of k_d^i([Kr], [He (Ar)]) was used to determine the rate constants of plasma-chemical reactions (1), (2), (5), (6) and the upper bound (up to an unknown value $k_4 m$) of the rates of reactions (3) and (7). The values of the rate constants k_1, k_2, k_3 and k_5, k_6, k_7, presented in Tables 1 and 2 were calculated by the least-squares method with the use of the Levenberg–Marquardt algorithm by varying the sought-for constants in relations

$$k_d^i = k_{1(5)}[Kr][He(Ar)] + k_{2(6)}[He(Ar)]^2 + k_{3(7)}[He(Ar)] \quad (24)$$

simultaneously for the entire set (for a given buffer gas) of the experimental values of k_d^i. The essence of the procedure was to construct in the coordinates ([Kr], [He (Ar)]) a curved surface

$$S([Kr], [He(Ar)]) = k_{1(5)}[Kr][He(Ar)] + k_{2(6)}[He(Ar)]^2 + k_{3(7)}[He(Ar)], \quad (25)$$

having the smallest deviation, in terms of the method, from the set of the experimental points (see details in [5]).

Note that the processing of the experimental dependence of $\ln\ln[1/T(t)]$ with the use of a simple linear approximation (20) shows that this representation is badly suited for the experimental situation. Calculations performed with the use of (20) allowed us to determine the rate constants of reactions (1), (5) and (3), (7) with very limited accuracy, which means that they can be considered only as an upper bound $k_{1(5)}^{upp}$ and $k_{3(7)}^{upp}$ (Tables 1 and 2). However, these calculations make it impossible to find quantitative values for the rate constants of reactions (2) and (6).

The results obtained in the present study show that under these experimental conditions, as in [3, 4], the collisional

Table 1. Upper bounds (k_i^{upp}) and average reaction rate constants (k_i) of the collisional quenching of the Kr atom in the $5s[3/2]_2^o$ state for the He–Kr mixture.

Reaction	k_i^{upp}	k_i	Reaction
(1)	3.1×10^{-33} cm^{6}s^{-1}	$(2.88\pm0.29)\times10^{-33}$ cm^{6}s^{-1}	this paper
(2)	–	$(4.6\pm1.3)\times10^{-36}$ cm^{6}s^{-1}	this paper
(3)	4.7×10^{-15} cm^{3}s^{-1}	$(1.51\pm0.15)\times10^{-15}$ cm^{3}s^{-1}	this paper

Table 2. Same as in Table 1 for the Ar–Kr mixture.

Reaction	k_i^{upp}	k_i	References
(5)	4.0×10^{-33} cm^{6}s^{-1}	$(4.10\pm0.25)\times10^{-33}$ cm^{6}s^{-1}	[3]
		$(3.56\pm0.36)\times10^{-33}$ cm^{6}s^{-1}	[4]
		$(3.48\pm0.35)\times10^{-33}$ cm^{6}s^{-1}	this paper
(6)	–	$(1.0\pm0.04)\times10^{-33}$ cm^{6}s^{-1}	[14]
		$<10^{-35}$ см^6/с	[3]
		$(5.9\pm0.8)\times10^{-36}$ cm^{6}s^{-1}	[4]
		$(5.7\pm0.9)\times10^{-36}$ cm^{6}s^{-1}	this paper
(7)	6.7×10^{-15} cm^{3}s^{-1}	$(0.69\pm0.06)\times10^{-15}$ cm^{3}s^{-1}	[14]
		$(1.1\pm0.1)\times10^{-15}$ cm^{3}s^{-1}	[15]
		$(3.78\pm0.23)\times10^{-15}$ cm^{3}s^{-1}	[3]
		$(3.26\pm0.33)\times10^{-15}$ cm^{3}s^{-1}	[4]
		$(3.17\pm0.32)\times10^{-15}$ cm^{3}s^{-1}	this paper

quenching of 5s states of the Kr atom in He–Kr and Ar–Kr mixtures occurs during tree-particle reactions with the formation of a homonuclear dimer Kr_2^* (1) and during two-particle reactions (3) and (4). At the same time, the three-particle reaction (2) with the formation of a heteronuclear dimer $HeKr^*$ is not involved in the collisional quenching of Kr^*. The latter may be explained by the fact that the heteronuclear dimer obtained in reaction (2) is unstable due to its low binding energy [16], and rapidly decays into the initial components in inverse collision reactions. In this case, the measured effective rate constant of the $HeKr^*$ dimer formation is close to zero.

4. Conclusions

We have studied for the first time the processes of deactivation of the metastable $Kr^*(5s[3/2]_2^o)$ state in He–Kr-mixtures, which are similar in composition and pressure to the mixtures used in excimer lasers and high-pressure lasers on atomic transitions in inert gases. It has been shown that the main channels of deactivation of this state are the processes of excimerisation with the formation of a Kr*2 dimer with a rate constant of 2.88×10^{-33} cm^6 s^{-1} and buffer gas quenching with a rate constant of 1.51×10^{-15} cm^3 s^{-1}. At the same time, reactions with the formation of heteronuclear dimers virtually play no noticeable role.

By increasing the amount of statistical data we have refined the rate constants of similar reactions for Ar–Kr mixtures, which within the measurement accuracy correspond to the values obtained by us for the first time in papers [3, 4].

Acknowledgements. The authors thank N.N. Ustinovskii for cooperation and useful discussions.

References

1. Zayarnyi D.A., Kholin I.V. *Kvantovaya Elektron.*, **33** (6), 474 (2003) [*Quantum Electron.*, **33** (6), 474 (2003)].
2. Semenova L.V., Ustinovskii N.N., Kholin I.V. *Kvantovaya Elektron.*, **34** (3), 189 (2004) [*Quantum Electron.*, **34** (3), 189 (2004)].
3. Zayarnyi D.A., L'dov A.Yu., Kholin I.V. *Kvantovaya Elektron.*, **39** (9), 821 (2009) [*Quantum Electron.*, **39** (9), 821 (2009)].
4. Zayarnyi D.A., L'dov A.Yu., Kholin I.V. *Kvantovaya Elektron.*, **40** (2), 144 (2010) [*Quantum Electron.*, **40** (2), 144 (2010)].
5. Zayarnyi D.A., L'dov A.Yu., Kholin I.V. *Kvantovaya Elektron.*, **41** (2) (2011) [*Quantum Electron.*, **41** (2) (2011)].
6. Kholin I.V. *Kvantovaya Elektron.*, **33** (2), 129 (2003) [*Quantum Electron.*, **33** (2), 129 (2003)].
7. Dudin A.Yu., Zayarnyi D.A., Semenova L.V., Ustinovskii N.N., Kholin I.V., Chugunov A.Yu. *Kvantovaya Elektron.*, **18** (8), 921 (1991) [*Sov. J. Quantum Electron.*, **21** (8), 833 (1991)].
8. Zvereva G.N., Lomaev M.I., Rybka D.V., Tarasenko V.F. *Opt. Spektrosk.*, **102** (1), 36 (2007).
9. Zayarnyi D.A., L'dov A.Yu., Ustinovskii N.N., Kholin I.V. *Prib. Tekh. Eksp.*, (4), 102 (2010).
10. Oka T. *Res. Rep. Nagaoka Thsh. Coll.*, **13** (4), 207 (1977).
11. Davis C.C., McFarlane R.A. *J. Quant. Spectrosc. Radiat. Transfer*, **18**, 151 (1977).
12. Zayarnyi D.A., Kholin I.V., Chugunov A.Yu. *Kvantovaya Elektron.*, **22** (3), 233 (1995) [*Quantum Electron.*, **25** (3), 217 (1995)].
13. Demidenko E.Z. *Optimizatsiya i regressiya* (Optimisation and Regression) (Moscow: Nauka, 1989).
14. Kolts J.H., Setser D.W. *J. Chem. Phys.*, **68** (11), 4848 (1978).
15. Sobczynski R., Setser D.W. *J. Chem. Phys.*, **95** (5), 3310 (1991).
16. Nowak G., Fricke J. *J. Phys. B: At. Mol. Phys.*, **18**, 1355 (1985)